2016-05-11

Molecular clusters Cs3X3 and Cs4X4 (X = Br, I): Quantum chemical study of structure and thermodynamic properties

Mwanga, Stanley F.

Cogent OA

Provided with love from The Nelson Mandela African Institution of Science and Technology

THEORETICAL & COMPUTATIONAL CHEMISTRY | RESEARCH ARTICLE

Molecular clusters Cs_3X_3 and Cs_4X_4 (X = Br, I): Quantum chemical study of structure and thermodynamic properties

Stanley F. Mwanga[1*], Tatiana P. Pogrebnaya[1] and Alexander M. Pogrebnoi[1]

*Corresponding author: Stanley F. Mwanga, Department of Materials Science and Engineering, The Nelson Mandela African Institution of Science and Technology (NM-AIST), P.O. Box 447, Nelson Mandela Rd, Tengeru, Arusha, Tanzania
E-mail: ferdinands@nm-aist.ac.tz

Abstract: The properties of trimer Cs_3X_3 and tetramer Cs_4X_4 (X = Br, I) molecules have been studied using DFT with B3LYP5 functional and MP2 and MP4 methods. Two equilibrium geometrical structures of trimers, hexagonal (D_{3h}) and "butterfly-shaped" (C_s), and one for tetramers, distorted cubic (T_d), are confirmed to exist; geometrical parameters and vibrational spectra are determined. The relative concentration of Cs_3X_3 isomers has been evaluated; the butterfly-shaped isomer dominates over hexagonal in saturated vapour in a broad temperature range. The dissociation reactions through different channels have been considered and enthalpies of formation $\Delta_f H°(0)$ of clusters determined: -858 ± 20 kJ mol^{-1} (Cs_3Br_3), -698 ± 20 kJ mol^{-1} (Cs_3I_3), -1270 ± 30 kJ mol^{-1} (Cs_4Br_4) and -1045 ± 30 kJ mol^{-1} (Cs_4I_4). The Gibbs free energies $\Delta_r G°(T)$ calculated for the dissociation reactions of trimer and tetramer molecules have indicated that these molecules are resistive in narrow temperature range only and decompose spontaneously with temperature increase with elimination of dimer molecules.

Subjects: Materials Science; Nanoscience & Nanotechnology; Physics

Keywords: DFT; MP2; MP4; molecular cluster; isomer; relative concentration; enthalpy of dissociation reaction and enthalpy of formation

ABOUT THE AUTHORS

Stanley F. Mwanga is a PhD student in Materials Science and Engineering at NM-AIST.

Professor Tatiana Pogrebnaya leads the computation chemistry group at the Nelson Mandela African Institution of Science and Technology (NM-AIST) in Arusha, Tanzania.

Alexander Pogrebnoi is a professor and lecturer; his research interests include material science, thermodynamics, high temperature mass spectrometry and quantum chemistry. The group is focused on quantum chemical study of inorganic and organic molecular and ionic clusters relating to fundamental research and practical applications in different areas. We investigate structure, vibrational and electronic spectra, thermodynamic properties of the species and energetics of chemical reactions.

Tatiana P. Pogrebnaya

PUBLIC INTEREST STATEMENT

Despite the seeming simplicity of alkali halide compounds, the composition of vapour over their solid or liquid surfaces appeared to be rather complex. Various molecular and ionic clusters were detected using mass spectrometric technique. The structure and properties of the clusters are not comprehended entirely by now. Quantum chemistry being a powerful instrument provides valuable knowledge about structure, spectra and thermodynamic properties of the species. In this work, we studied the trimer and tetramer clusters of caesium halides using the quantum chemical methods. Besides the structural properties of the species their thermodynamic stability regarding different decomposition routes is analysed. These results may be useful in industrial applications, e.g. in halogen metallurgy, manufacture of modern electronic devices, halogen lamps, chemical vapour transport and deposition.

1. Introduction

The study of alkali halide clusters, ionic and molecular, has been the subject of research over past five decades. This involves both experimental (Butman, Kudin, Smirnov, & Munir, 2000; Chupka, 1959; Dunaev, Kudin, Butman, & Motalov, 2013; Gusarov, 1986; Pogrebnoi, Kudin, & Kuznetsov, 2000; Sidorova, Gusarov, & Gorokhov, 1979; Snelson, 1967) and theoretical (Cohen & Gordon, 1975; Rupp & Ahlrichs, 1977; Weis, Ochsenfeld, Ahlrichs, & Kappes, 1992; Welch, Lazareth, Dienes, & Hatcher, 1976) studies. Most experimental studies have dealt with the identification of cluster species existing in saturated vapour and measurement of equilibrium constants of ion molecular reactions. On the other hand theoretical studies concern mainly prediction of equilibrium configurations, geometrical parameters, binding energies and vibrational frequencies. These clusters are of interest because they have unique electronic, optical and magnetic properties which make them to be useful in different applications. For example, caesium chloride thin films were used in fabrication of electronic devices through ion implantation techniques (Lee, Han, Choi, & Moon, 2010; Liao, Liu, Wang, & Yi, 2011; Liu, Ashmkhan, Dong, Wang, & Yi, 2013; Liu, Ferguson, Yavuz, & Cui, 2012; Zhang, Liu, Wang, Zhang, & Yi, 2014; Zhang et al., 2012). Cluster ions have been proved to be useful in ionic thrusters (Benson & Patterson, 2009) and magneto-hydrodynamic generators (Kay, 2011). Besides, caesium and iodine exist among the fission products that may be released in nuclear power plants (Badawi, Xerri, Canneaux, Cantrel, & Louis, 2012; Lennart & Kjell, 1994; Povinec et al., 2013; Roki, Ohnet, Fillet, Chatillon, & Nuta, 2013, 2014); these by-products are highly radioactive materials. Thus, evaluations of thermodynamic properties of gaseous species are essential for safety features of a nuclear pressurized reactor. The thermodynamic functions of gaseous species are usually derived by statistical thermodynamics from the geometrical parameters and vibrational frequencies.

Recently, we have theoretically investigated the properties of molecular and ionic clusters of caesium fluoride (Mwanga, Pogrebnaya, & Pogrebnoi, 2015a), caesium chloride (Hishamunda, Girabawe, Pogrebnaya, & Pogrebnoi, 2012; Pogrebnaya, Hishamunda, Girabawe, & Pogrebnoi, 2012) and caesium bromide and iodide (Mwanga, Pogrebnaya, & Pogrebnoi, 2015b). In these works, the equilibrium geometrical structure, vibrational spectra and thermodynamic properties of the clusters were determined. The dimers and trimers of caesium bromine and iodine have been studied theoretically and experimentally by Groen and Kovács (2010). Molecular clusters of lithium iodide have been found to exist in vapour over solid lithium iodide (Bencze, Lesar, & Popovic, 1998). However, tetramers of caesium bromide and iodine have not yet studied. We also anticipate that isomeric forms would exist for trimers of caesium bromine and iodine as it was revealed for caesium fluoride and chloride (Mwanga et al., 2015a; Mwanga, Pogrebnaya, & Pogrebnoi, 2016). In this work, we present quantum chemical investigation of the properties of trimer Cs_3X_3 and tetramer Cs_4X_4 (X = Br, I) molecules.

2. Computational details

Quantum chemical calculations are performed using General Atomic and Molecular Electronic Structure System (GAMESS) (Schmidt et al., 1993) software package, Firefly version 8.1.0 (Granovsky, 2012). Electron density functional theory (DFT) with the Becke–Lee–Yang–Parr functional (B3LYP5) (Becke, 1993; Lee, Yang, & Parr, 1988) and second and fourth order Møller–Plesset perturbation theory (MP2 and MP4) have been used. The relativistic effective core potential ECP GEN 46 3 with basis set Def2-QZVP 6s5p4d1f for caesium (Leininger et al., 1996) is used. For bromine and iodine atoms, relativistic ECP GEN 28 4, 7 electrons in the core (Br) and ECP GEN 46 4, 7 electrons in the core (I) with SDB-aug-cc-pVTZ basis sets 4s4p3d2f (Martin & Sundermann, 2001) have been applied. These basis sets were accessed from EMSL (Schuchardt et al., 2007). The geometry of the species was optimized by B3LYP5 and MP2 methods. We expect that including the diffused functions into valence basis sets of halogen atoms, Br and I, will improve an accuracy of the calculated thermochemical properties of the species as it is based on results by Martin and Sundermann (2001) and our experience as well (Mwanga et al., 2015a). A vibrational analysis was performed at the same level of calculations to examine whether the obtained structure corresponds to a real energy minimum by the absence of the imaginary frequencies. The visualization of geometrical structure and vibrational spectra the software have been used: MacMolPlt (Bode & Gordon, 1998) and Chemcraft ("Chemcraft. Version 1.7 (build 132). G. A. Zhurko, D. A. Zhurko. HTML" (Zhurko & Zhurko, 2014).

The enthalpies of the chemical reactions $\Delta_r H°(0)$ were calculated on the basis of energies $\Delta_r E$, and the zero-point vibration energy (ZPVE) correction $\Delta_r \varepsilon$ as given in following equations:

$$\Delta_r H°(0) = \Delta_r E + \Delta_r \varepsilon \tag{1}$$

$$\Delta_r \varepsilon = \frac{1}{2} hc \left(\sum \omega_{iprod} - \sum \omega_{ireact} \right) \tag{2}$$

where h is the Planck constant, c is the speed of light in the free space, $\sum \omega_{iprod}$ and $\sum \omega_{ireact}$ are the sums of the vibrational frequencies of the products and reactants, respectively. This approach is similar to that applied by Curtiss, Redfern, and Frurip (2000).

The dissociation energies $\Delta_r E$ of the species were calculated by B3LYP5 and MP2 methods, MP4 was employed using the optimized coordinates determined by MP2 method. The correction for basis set superposition error (BSSE) (Boys & Bernardi, 1970) has been employed for MP2 and MP4 as well using procedure proposed by Solomonik and co-workers (Solomonik, Smirnov, & Mileev, 2005). In the DFT calculations, BSSE correction was not considered. According to Liu, Zhao, Li, and Chen (2013) as well as our previous work (Mwanga et al., 2015a), the DFT methods are not mush sensitive to the BSSE correction and the latter does not improve the DFT results on energies and enthalpies of dissociation reactions.

3. Results and discussion

3.1. Trimer Cs_3Br_3 and Cs_3I_3 molecules

For trimer Cs_3X_3 molecules, two equilibrium structures were confirmed to have minima at the potential energy surface (PES): hexagonal planar (D_{3h}) and butterfly-shaped (C_s) (Figure 1(a and b)). The geometrical parameters and vibrational spectra of these structures are compiled in Tables 1 and 2. As expected, there is a progressive increase in internuclear separation from bromide to iodide. Regarding the energy, butterfly-shaped isomer possesses lower energy by ~14 kJ mol^{-1} (Cs_3Br_3) and ~15 kJ mol^{-1} (Cs_3I_3) than hexagonal (MP2). Thus, butterfly-shaped structure is more energetically stable than hexagonal. Similar isomeric forms were confirmed to exist for Cs_3F_3 and Cs_3Cl_3 in our previous works (Mwanga et al., 2015a, 2016), respectively. We have evaluated the energy barrier in the path from the C_s ("butterfly") to D_{3h} (hexahonal) configuration. In the molecule within C_s symmetry, the separation between two opposite atoms, Cs_2–X_2 (Figure 1(b)), was a variable parameter (transition reaction coordinate). This parameter was varied with a step of 0.5 Å from the distance in the C_s structure up to that in the hexagonal one. All other atom coordinates were optimized at each step. It was revealed that the barrier for the transition was ~6 kJ mol^{-1} both for Cs_3Br_3 and Cs_3I_3 (DFT/ B3LYP5). Heat energy of the molecules at ~350 K is ~3 kJ mol^{-1}, which is twice less compared to the barrier. The barrier also is much higher regarding vibrational energy quantum, that is ~1 kJ mol^{-1}.

The vibrational frequencies determined by B3LYP5 and MP2 methods are given in Tables 1 and 2. In most cases, a good agreement is observed between the corresponding frequencies found by two methods. Based on our previous experience (Mwanga et al., 2015a, 2015b, 2016) we consider that MP2 results to be more applicable for further consideration and calculation of the thermodynamic

Figure 1. Geometrical structures of the trimers Cs_3X_3 and tetramer Cs_4X_4 (X = Br, I) molecules: (a) Cs_3X_3, planar hexagonal D_{3h}; (b) Cs_3X_3, butterfly-shaped C_s; (c) Cs_4X_4, distorted cube T_d.
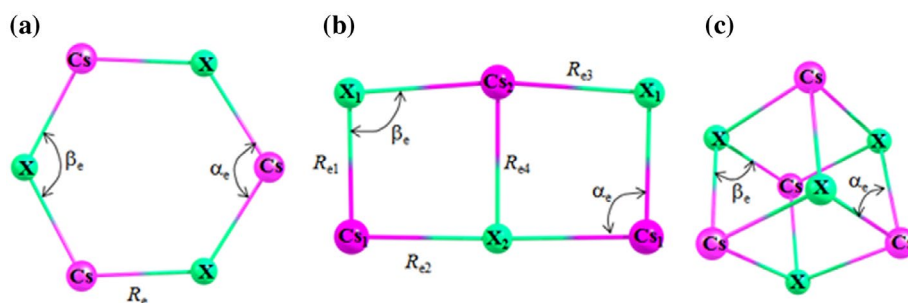
Table 1. Properties of neutral molecules Cs_3X_3 (hexagonal, D_{3h}), X = Br, I				
Property	**Cs_3Br_3 (D_{3h})**		**Cs_3I_3 (D_{3h})**	
	B3LYP5	**MP2**	**B3LYP5**	**MP2**
R_e(Cs−X)	3.377	3.348	3.626	3.589
α_e(X−Cs−X)	119.3	117.9	123.2	121.8
β_e(Cs−X−Cs)	120.7	122.1	116.8	118.2
$-E$	100.84946	100.43294	94.95303	94.49097
ω_1 (A_1')	103 (0)	114 (0)	86 (0)	91 (0)
ω_2 (A_1')	68 (0)	86 (0)	58 (0)	59 (0)
ω_3 (A_1')	33 (0)	43 (0)	28 (0)	28 (0)
ω_4 (A_2'')	26 (0.61)	26 (0.63)	22 (0.44)	23 (0.46)
ω_5 (E')	110 (1.22)	118 (1.1)	88 (0.97)	91 (0.95)
ω_6 (E')	85 (0.28)	91 (0.06)	71 (0.01)	73 (0.00)
ω_7 (E')	19 (0.24)	12 (0.22)	12 (0.09)	12 (0.08)
ω_8 (E'')	12 (0)	12 (0)	11 (0)	11 (0)
q(Cs)	0.834	0.881	0.800	0.860
q(X)	−0.834	−0.881	−0.800	−0.860

Notes: Here and hereafter R_e(Cs−X) is the equilibrium internuclear distance, Å; α_e(X−Cs−X) and β_e(Cs−X−Cs) are valence angles, degs; E is the total electron energy, au; ω_i are vibrational frequencies, cm^{-1}; the values given in parentheses near the frequencies are IR intensities, D^2 amu^{-1} Å^{-2}.

functions of the species. The decrease in the corresponding values of ω_i is observed from bromide to iodide. Several low frequencies of ~30 cm^{-1} and less are found in spectra of both isomers of Cs_3X_3: there are $\omega_3, \omega_4, \omega_7, \omega_8$ for hexagonal isomer and $\omega_5, \omega_6, \omega_7, \omega_{11}, \omega_{12}$ for C_s isomer. The assignments of vibrational frequencies for Cs_3X_3 are presented in Figures 2 and 3. As for hexagonal planar Cs_3X_3, both species have few modes active in IR spectra, Cs–X stretching being the highest intensity. The bands of medium intensity are wagging X–Cs–X modes with low frequencies, 26 cm^{-1} (Cs_3Br_3) and 23 cm^{-1} (Cs_3I_3). The bands of weak intensity are related to rocking Cs–X–Cs vibrations with low vibration frequency of 12 cm^{-1}. Our computed vibrational spectra for Cs_3X_3 (D_{3h}) can be compared with experimental data in Groen and Kovács (2010) where FT-IR spectra of $(CsBr)_n$ and $(CsI)_n$ (n = 1–3) had been measured using matrix isolation technique. For the trimers, the vibrational modes 110.2 cm^{-1} in Kr and 103.1 cm^{-1} in Xe matrix for Cs_3Br_3 and 86.6 cm^{-1} in Xe for Cs_3I_3 had been recorded. Therefore our values, 118 cm^{-1} (Cs_3Br_3) and 91 cm^{-1} (Cs_3I_3), agree well with the experimental frequencies. Worth to note also that our results for the trimer molecules are in a good agreement with theoretical data (Groen & Kovács, 2010).

For butterfly-shaped isomers, the majority of vibrational modes are active in IR spectra although most of them have weak intensity. The bands of highest intensity correspond to Cs–X stretching vibrations; the most intensive bands are observed at 118 cm^{-1} (Cs-Br) and 93 cm^{-1} (Cs-I). Other valence vibrations at 67 cm^{-1} (Cs_3Br_3) and 63 cm^{-1} (Cs_3I_3) possess low intensities. The bending vibrational modes are characterized by weak intensities.

To consider the electron density distribution, we have calculated the Mullikan atomic charges q by both methods, DFT and MP2 (Tables 1 and 2). One can see the high ionicity of the species as the charges on atoms are about 0.8–0.9 au. For both isomers of Cs_3Br_3 and Cs_3I_3, the MP2 method demonstrates higher ionicity as the charge magnitudes are bigger by 0.03–0.07 au than the corresponding values of q obtained by DFT. It is worth to mention here the dipole moments μ_e as they relate to the electron density distribution (Table 2). The values of μ_e also demonstrate that the DFT method underrates the ionic character of bonds as μ_e(DFT) < μ_e(MP2). It is evident that this correlation holds due to charges relationship, q(DFT) < q(MP2). On comparing two isomers, in the hexagonal one of

cogent · chemistry

Table 2. Properties of neutral molecules Cs$_3$X$_3$ ("butterfly-shaped", C_s), X = Br, I				
Property	**Cs$_3$Br$_3$ (C_s)**		**Cs$_3$I$_3$ (C_s)**	
	B3LYP5	**MP2**	**B3LYP5**	**MP2**
R_{e1}(Cs$_1$–X$_1$)	3.303	3.264	3.553	3.517
R_{e2}(Cs$_1$–X$_2$)	3.429	3.374	3.680	3.615
R_{e3}(Cs$_2$–X$_1$)	3.487	3.431	3.734	3.674
R_{e4}(Cs$_2$–X$_2$)	3.737	3.606	3.986	3.842
α_e(X$_1$–Cs$_1$–X$_2$)	94.0	92.0	96.5	94.3
β_e(Cs$_1$–X$_1$–Cs$_2$)	93.2	93.7	90.2	90.8
χ_e(Cs$_1$–X$_2$–Cs$_2$–X$_1$)	169.0	169.8	172.0	173.1
–E	100.85067	100.43813	94.95448	94.49674
$\Delta_r E_{iso}$	–3.19	–13.63	–3.82	–15.15
ω_1 (A′)	109 (1.05)	118 (1.01)	85 (1.00)	93 (0.72)
ω_2 (A′)	90 (0.34)	101 (0.36)	75 (0.12)	86 (0.08)
ω_3 (A′)	62 (0.10)	67 (0.14)	53 (0.06)	59 (0.07)
ω_4 (A′)	44 (0.12)	61 (0.12)	39 (0.11)	50 (0.08)
ω_5 (A′)	35 (0.03)	37 (0.23)	27 (0.08)	30 (0.08)
ω_6 (A′)	29 (0.29)	31 (0.26)	24 (0.24)	26 (0.30)
ω_7 (A′)	5 (0.01)	10 (0.01)	6 (0.00)	7 (0.01)
ω_8 (A″)	112 (0.60)	120 (0.75)	89 (0.77)	95 (0.79)
ω_9 (A″)	104 (0.62)	110 (0.41)	88 (0.00)	93 (0.21)
ω_{10} (A″)	79 (0.02)	86 (0.01)	56 (0.02)	63 (0.03)
ω_{11} (A″)	34 (0.10)	36 (0.10)	27 (0.13)	28 (0.08)
ω_{12} (A″)	16 (0.00)	16 (0.00)	13 (0.00)	13 (0.00)
μ_e	9.92	10.45	10.68	11.31
q(Cs$_1$)	0.814	0.868	0.776	0.851
q(X$_1$)	–0.834	–0.882	–0.778	–0.853
q(Cs$_2$)	0.850	0.880	0.776	0.837
q(X$_2$)	–0.811	–0.852	–0.772	–0.833

Note: χ_e(Cs1–X2–Cs2–X1) is the dihedral angle, degs; $\Delta_r E_{iso} = E(Cs_3X_3, C_s) − E(Cs_3X_3, D_{3h})$ is isomerization energy, kJ mol^{-1}; μ_e is the dipole moment, D.

Cs$_3$X$_3$ the absolute values of charges on X and Cs atoms are equal which follows from the high symmetry of the structure. In the isomers of C_s configuration, the electron density distribution is not uniform: according to MP2 results, the side caesium atoms, Cs$_1$, have slightly smaller charges (by 0.01 au) than the middle Cs$_2$ atom, while the side halogen atoms X$_1$ have bigger charge magnitudes (by ~0.02 au) compared to the middle one X$_2$, that holds for both Cs$_3$Br$_3$ and Cs$_3$I$_3$ clusters. Ionicity slightly decreases, by 0.01–0.02 au, from the hexagonal to "butterfly" configuration and from bromide to iodide.

The relative concentration p_{II}/p_I of the isomers in the saturated vapour was evaluated using the following formula:

$$\Delta_r H°(0) = T\Delta_r \Phi°(T) - RT \ln\left(\frac{p_{II}}{p_I}\right) \tag{3}$$

where $\Delta_r H°(0)$ is the enthalpy of the isomerization reaction Cs$_3$X$_3$ (D_{3h}) → Cs$_3$X$_3$ (C_s); T is absolute temperature; p_I is the partial pressure of the D_{3h} isomer, and p_{II} is that of C_s one; $\Delta_r \Phi°(T)$ is the reduced Gibbs energy of the reaction, $\Delta_r \Phi°(T) = \Phi°(T)_{prod} - \Phi°(T)_{react}$. The value of $\Phi°(T)$ comprises the enthalpy

✳️ **cogent** ·· chemistry

Figure 2. IR spectrum of planar hexagonal isomer Cs_3X_3 (D_{3h}): (a) Cs_3Br_3 and (b) Cs_3I_3.
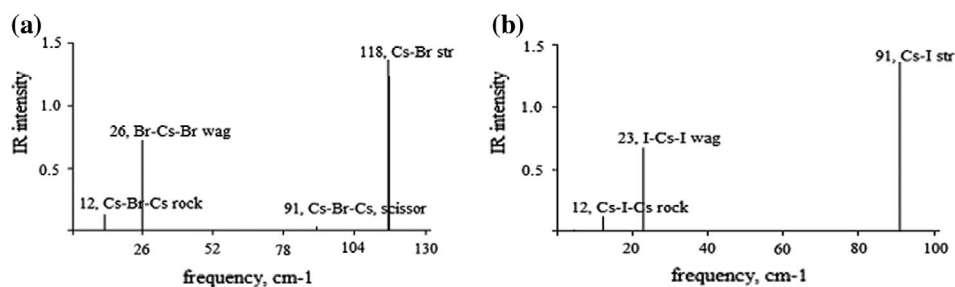
Figure 3. IR spectrum of butterfly-shaped isomer Cs_3X_3 (C_s): (a) Cs_3Br_3 and (b) Cs_3I_3.
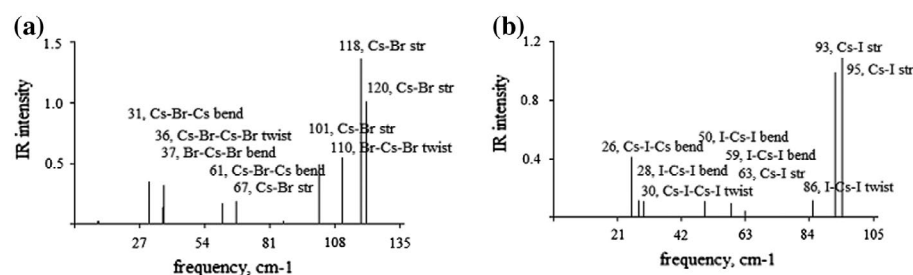
increment [$H°(T) − H°(0)$] and entropy $S°(T)$ of each species: $Φ°(T) = −[H°(T) − H°(0) − TS°(T)]/T$. The values of $Φ°(T)$ and other thermodynamic functions were calculated using OpenThermo software (Tokarev, 2007–2009) within the "rigid rotator-harmonic oscillator" approximation; the optimized coordinates and vibrational frequencies obtained by MP2 method were used as the input parameters. The enthalpies of the isomerization reactions $Δ_rH°(0)$ were calculated on the basis of isomerization energies $Δ_rE_{iso}$ using Equations (1 and 2). The isomerization energies $Δ_rE_{iso}$, ZPVEs $Δ_rε$, enthalpies $Δ_rH°(0)$ of isomerization reactions, change in the reduced Gibbs energies $Δ_rΦ°(T)$, and the relative abundance p_{II}/p_I of the isomers at $T = 500$ K are presented in Table 3. The value of p_{II}/p_I indicates which of the isomers prevails in saturated vapour. For both species, the butterfly-shaped Cs_3X_3 (C_s) dominates over hexagonal-shaped Cs_3X_3 (D_{3h}) isomer, as the ratio p_{II}/p_I is greater than one.

The temperature effect on the relative abundance p_{II}/p_I of the isomers is considered for temperature range between 300 and 700 K (Figure 4). As is seen, the relative concentration of the butterfly-shaped isomer at 300 K is ~80 for Cs_3Br_3 and ~200 for Cs_3I_3, and decreases with temperature rise being still greater than one. Worth to note that the relative abundance of isomers is influenced by two factors, the isomerization energy and entropy $S°$ of species: the lower is the $Δ_rE_{iso}$, and bigger $S°$ of the isomer II, the higher is the ratio p_{II}/p_I. Thus, being favoured by both of these factors, the isomer with C_s symmetry is predicted to dominate in vapour in a broad temperature range.

The enthalpies of dissociation reactions $Δ_rH°(0)$ with the elimination of CsX molecules and enthalpies of formation $Δ_fH°(0)$ of Cs_3X_3 were calculated for the C_s isomer based on MP4C results. The values of $Δ_fH°(0)$ for CsX and Cs_2X_2 molecules were taken from (Gurvich et al., 2000). The theoretical values of $Δ_rH°(0)$ were calculated using Equations (1 and 2).

Table 3. The energies $Δ_rE_{iso}$ and enthalpies $Δ_rH°(0)$ of the isomerization reactions, change in the reduced Gibbs free energies $Δ_rΦ°(T)$, ZPVE corrections $Δ_rε$ and relative abundances p_{II}/p_I of the isomers ($T = 500$ K)

Isomerization reaction	$Δ_rE_{iso}$, kJ mol⁻¹	$Δ_rε$, kJ mol⁻¹	$Δ_rH°(0)$, kJ mol⁻¹	$Δ_rΦ°(T)$, J mol⁻¹ K⁻¹	p_{II}/p_I
Cs_3Br_3 (D_{3h}) = Cs_3Br_3 (C_s)	−13.63	0.35	−13.28	−8.118	9.2
Cs_3I_3 (D_{3h}) = Cs_3I_3 (C_s)	−15.15	0.41	−14.74	−5.032	18.9

Figure 4. Temperature dependence of the relative concentration of the isomers for trimers Cs$_3$X$_3$ (X = Br, I) molecules.
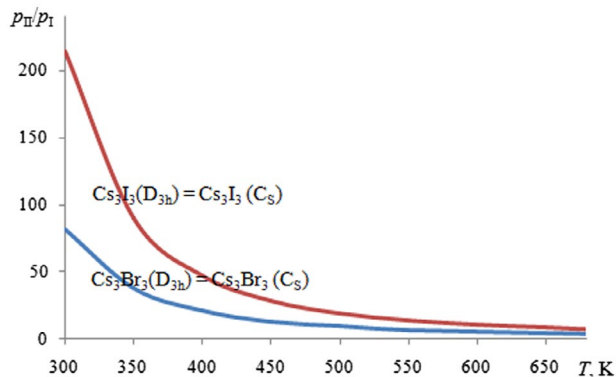
It is worth to note that the spin–orbit coupling effect may be important for heavy atoms, especially for species with two or more low lying electronic states (Fedorov, Koseki, Schmidt, & Gordon, 2003). In our case the first excited electronic state is far above the ground state, according to the TDDFT calculations, the first excitation energies are ~4.5 eV (Cs$_3$Br$_3$) and ~4.1 eV (Cs$_3$I$_3$). Therefore, the spin–orbit coupling was not taken into account in calculation of thermodynamic properties.

The calculated dissociation energies $\Delta_r E$, ZPVE corrections $\Delta_r \varepsilon$, enthalpies of the dissociation reactions $\Delta_r H°(0)$, and enthalpies of formation $\Delta_f H°(0)$ of Cs$_3$X$_3$ molecules are presented in Table 4. The data determined previously for Cs$_3$F$_3$ (Mwanga et al., 2015a) and Cs$_3$Cl$_3$ (Mwanga et al., 2016) are included for comparison. Two types of dissociation reactions are considered: (i) into monomer and dimer and (ii) into three monomers. From fluoride to iodide the enthalpies of the dissociation reactions decrease: 129→121→117→110 kJ mol^{-1} for the reactions (i), and 301→276→267→253 kJ mol^{-1} for the reactions (ii). The second type of reactions requires approximately 2.3 times bigger energy than first one due to different number of bonds to be broken. The uncertainties of the $\Delta_r H°(0)$ values may be estimated on the base of the comparison between theoretical and experimental data available for Cs$_2$Br$_2$, Cs$_2$I$_2$, Cs$_3$I$_2^+$, Cs$_2$I$_3^-$ (Mwanga et al., 2015b) and Cs$_4$Cl$_3^+$ (Mwanga et al., 2016) for which the maximum difference between the calculated MP4C method and experimental was equal to 16 kJ mol^{-1}. The enthalpies of formation $\Delta_f H°(0)$ of the trimers found through both types of reactions are close to each other or coincide. The uncertainty is accepted to be ± 20 kJ mol^{-1}, and the values of $\Delta_f H°(0)$ are as follows: −858 ± 20 kJ mol^{-1} (Cs$_3$Br$_3$) and −698 ± 20 kJ mol^{-1} (Cs$_3$I$_3$).

Table 4. The energies, $\Delta_r E$, ZPVE corrections, $\Delta_r \varepsilon$, and enthalpies $\Delta_r H°(0)$ of the dissociation reactions, and enthalpies of formation $\Delta_f H°(0)$ of Cs$_3$X$_3$ (C_s) (X = F, Cl, Br, I) molecules, all values are in kJ mol^{-1}

| No.	Dissociation reaction	$\Delta_r E$	$-\Delta_r \varepsilon$	$\Delta_r H°(0)$	$-\Delta_f H°(0)$
1	Cs$_3$F$_3$ = CsF + Cs$_2$F$_2$	130.9	1.57	129	1,378
2	Cs$_3$F$_3$ = 3CsF	304.7	4.22	301	1,386
3	Cs$_3$Cl$_3$ = CsCl + Cs$_2$Cl$_2$	121.4	1.16	121	996
4	Cs$_3$Cl$_3$ = 3CsCl	278.3	2.76	276	996
5	Cs$_3$Br$_3$ = CsBr + Cs$_2$Br$_2$	117.5	0.98	117	858
6	Cs$_3$Br$_3$ = 3CsBr	268.7	2.14	267	858
7	Cs$_3$I$_3$ = CsI + Cs$_2$I$_2$	111.0	0.93	110	698
8	Cs$_3$I$_3$ = 3CsI	254.6	1.95	253	698

Notes: The values of $\Delta_r E$ and $\Delta_r \varepsilon$ were obtained by MP4C and MP2 methods, respectively. The results for reactions 1–4 are based on our previous works (Mwanga et al., 2015a, 2016).

cogent · chemistry

Table 5. Properties of neutral molecules Cs_4X_4 (distorted cubic, T_d), X = Br, I

Property	Cs_4Br_4		Cs_4I_4	
	B3LYP5	MP2	B3LYP5	MP2
R_e(Cs–X)	3.512	3.433	3.768	3.678
α_e (X–Cs–X)	90.4	89.6	92.9	91.9
β_e(Cs–X–Cs)	89.6	90.4	87.1	88.0
$-E$	134.50200	133.96752	126.63848	126.04400
ω_1 (A_1)	89 (0)	83 (0)	53(0)	83 (0)
ω_2 (A_1)	46 (0)	31 (0)	36 (0)	36 (0)
ω_3 (E)	70 (0)	85 (0)	52 (0)	66 (0)
ω_4 (E)	35 (0)	35 (0)	24 (0)	37 (0)
ω_5 (T_1)	66 (0)	84 (0)	51 (0)	66 (0)
ω_6 (T_2)	89 (1.34)	95 (0.24)	66 (1.17)	82 (1.95)
ω_7 (T_2)	84 (2.66)	85 (3.75)	63 (1.59)	71 (0.71)
ω_8 (T_2)	36 (0.04)	19 (0.003)	26 (0.06)	26 (0.36)
q(Cs)	0.874	0.909	0.823	0.876
q(X)	−0.874	−0.909	−0.823	−0.876

3.2. Tetramers Cs_4Br_4 and Cs_4I_4 molecules

For the tetramers Cs_4X_4 molecules, only one equilibrium structure with T_d symmetry was confirmed to exist (Figure 1(c)). This structure is specified by two parameters R_e(Cs–X) and α_e(X–Cs–X). The geometrical parameters and vibrational frequencies of Cs_4X_4 molecules are gathered in Table 5. Similar to trimers, the internuclear separation increases from bromide to iodide, while the corresponding vibrational frequencies decrease as a rule. Due to compactness of the tetramer structure, the deformational frequencies are not so low compared to trimers, both hexagonal and "butterfly-shaped".

The IR spectra of Cs_4X_4 (T_d) are shown in Figure 5(a and b). One can see that only two modes are active: mode of high intensity at 85 cm^{-1} (Cs_4Br_4) and 82 cm^{-1} (Cs_4I_4) assigned to X–X wagging vibrations and the low intensive mode at 95 cm^{-1} (Cs_4Br_4) and 71 cm^{-1} (Cs_4I_4) which corresponds to Cs–X–Cs twisting vibrations.

The electron density distribution is represented through the Mullikan atomic charges q found by both methods, DFT and MP2 (Table 5). The values of q being about 0.8–0.9 au show a high ionic character of bonds. The observations discussed above for the trimer molecules are valid here as well; the magnitudes of q are higher by MP2 than DFT, the ionicity decreases from bromide to iodide. Compared to the trimer molecules, the charges in tetramers are slightly higher by 0.02–0.03 au.

Figure 5. Calculated IR spectra of distorted cube Cs_4X_4 (T_d): (a) Cs_4Br_4 and (b) Cs_4I_4.

✻cogent ·· chemistry
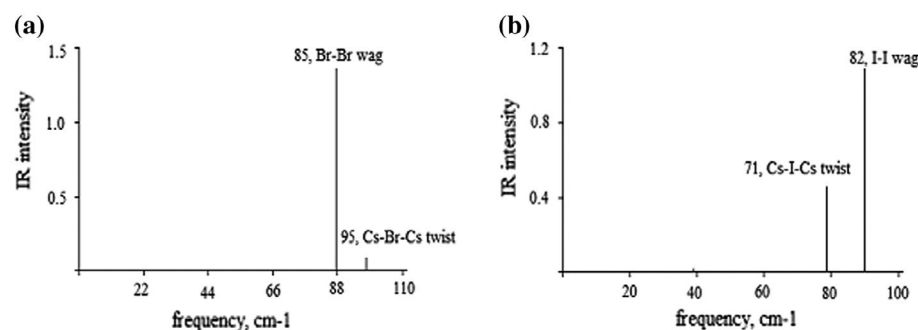
Table 6. The energies, $\Delta_r E$, ZPVE corrections, $\Delta_r \varepsilon$, and enthalpies $\Delta_r H°(0)$ of the dissociation reactions, and enthalpies of formation $\Delta_f H°(0)$ of Cs_4X_4 (T_d) (X = F, Cl, Br, I) molecules, all values are in kJ mol^{-1}

No.	Dissociation reaction	$\Delta_r E$	$-\Delta_r \varepsilon$	$\Delta_r H (0)$	$-\Delta_f H (0)$
1	$Cs_4F_4 = CsF + Cs_3F_3$	210.0	4.00	206	1,949
2	$Cs_4F_4 = 2Cs_2F_2$	169.8	2.66	167	1,941
3	$Cs_4F_4 = 4CsF$	517.4	7.96	509	1,956
4	$Cs_4Cl_4 = CsCl + Cs_3Cl_3$	219	2.15	217	1,453
5	$Cs_4Cl_4 = 2Cs_2Cl_2$	183.5	1.71	182	1,464
6	$Cs_4Cl_4 = 4CsCl$	497.3	4.9	492	1,453
7	$Cs_4Br_4 = CsBr + Cs_3Br_3$	213.0	3.43	210	1,265
8	$Cs_4Br_4 = 2Cs_2Br_2$	179.2	1.41	178	1,274
9	$Cs_4Br_4 = 4CsBr$	481.7	3.73	478	1,267
10	$Cs_4I_4 = CsI + Cs_3I_3$	192.6	1.81	191	1,038
11	$Cs_4I_4 = 2Cs_2I_2$	160.0	1.73	158	1,054
12	$Cs_4I_4 = 4CsI$	447.3	3.59	444	1,038

Notes: The values of $\Delta_r E$ and $\Delta_r \varepsilon$ were obtained by MP4C and MP2 methods, respectively. The results for reactions 1–6 are based on our previous works (Mwanga et al., 2015a, 2016).

Three channels of the dissociation of Cs_4X_4 molecules with the elimination of monomer and dimer molecules were considered (Table 6), similarly to trimers, the data of our previous works were included (Mwanga et al., 2015a, 2016). It can be observed the dissociation into two Cs_2X_2 molecules requires lowest energy than other two channels. For the dissociation into two dimers, the values of $\Delta_r H°(0)$ are less by 39 kJ mol^{-1} (Cs_4F_4), 35 kJ mol^{-1} (Cs_4Cl_4), 32 kJ mol^{-1} (Cs_4Br_4) and 33 kJ mol^{-1} (Cs_4I_4) compared to the dissociation into monomer plus trimer and by 342 kJ mol^{-1} (Cs_4F_4), 310 kJ mol^{-1} (Cs_4Cl_4), 300 kJ mol^{-1} (Cs_4Br_4) and 286 kJ mol^{-1} (Cs_4I_4) compared to the dissociation into four CsX molecules. Uncertainties of the enthalpies of reaction and enthalpies of formations were estimated as ±20 kJ mol^{-1} and ±30 kJ mol^{-1}, respectively. The enthalpies of formation found on the base of three reactions are close to each other, the averaged values of $\Delta_f H°(0)$ were accepted: −1270 ± 30 kJ mol^{-1} (Cs_4Br_4) and −1043 ± 30 kJ mol^{-1} (Cs_4I_4).

3.3. Trimer and tetramer dissociation: thermodynamic approach
For the most probable channels of dissociation of the clusters, the Gibbs free energies were calculated and plotted vs. temperature (Figures 6 and 7). The plots for other two halides, Cs_3X_3 and Cs_4X_4 (X = F and Cl) were included. As seen, the values of $\Delta_r G°$ are positive for rather narrow temperature range; the change of sign occurs at ~330 K, 280 K, 240 K and 210 K for Cs_3X_3 and ~390 K, 370 K, 360 K and 250 K for Cs_4X_4 (X = F, Cl, Br and I), respectively. Therefore, according to the thermodynamic approach, only Cs_3F_3 and all tetramers excluding Cs_4I_4 may exist at the room and moderate temperatures. With temperature rise, all trimers Cs_3X_3 dissociate spontaneously into CsX plus Cs_2X_2 while tetramers Cs_4X_4 decompose into two dimeric molecules.

Figure 6. Gibbs free energy change vs. temperature for the reaction $Cs_3X_3 = CsX + Cs_2X_2$ (X = F, Cl, Br and I).
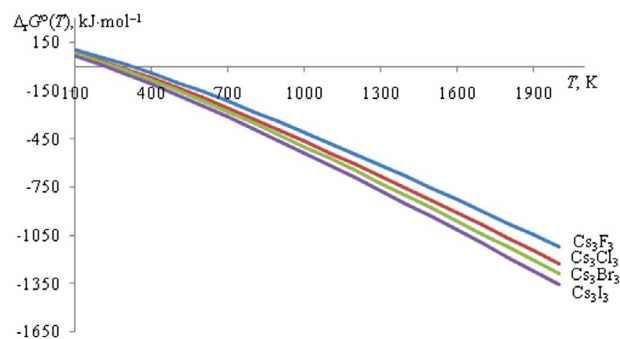
Figure 7. Gibbs free energy change vs. temperature for the reaction $Cs_4X_4 = 2Cs_2X_2$ (X = F, Cl, Br and I).
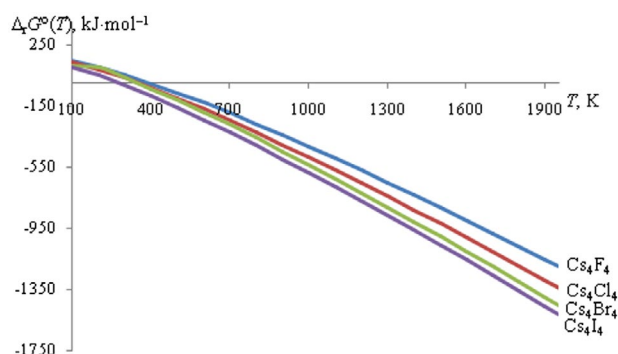
4. Conclusion

The geometrical structure and vibrational spectra of the trimer and tetramer molecules, Cs_3X_3 and Cs_4X_4 (X = Br and I), were determined by DFT/B3LYP5 and MP2 methods; the results were in a good accordance, as a rule, between each other and also with experimental and theoretical data available in literature. Regarding the enthalpies of dissociation reactions, the MP2 method was more preferable compared to DFT; the BSSE correction was to be taken into account. The existence of two isomeric forms, hexagonal and "butterfly-shaped", for Cs_3X_3 was confirmed, and the latter isomer was found to prevail in equilibrium vapour. Thermodynamic properties of Cs_3X_3 and Cs_4X_4 were calculated. Different dissociation channels were considered; among them the routes with elimination of dimeric molecules appeared to be most feasible. The analysis of Gibbs free energy $\Delta_r G°$ revealed that these clusters are not stable at elevated temperatures; at temperatures greater than ~400 K both Cs_3X_3 and Cs_4X_4 dissociate spontaneously into CsX plus Cs_2X_2 and two dimer molecules, respectively. Tetramers are more stable than trimers, likely due to compact cubic structure.

Author details

Stanley F. Mwanga[1]
E-mail: ferdinands@nm-aist.ac.tz
Tatiana P. Pogrebnaya[1]
E-mail: tatiana.pogrebnaya@nm-aist.ac.tz
Alexander M. Pogrebnoi[1]
E-mail: alexander.pogrebnoi@nm-aist.ac.tz
[1] Department of Materials Science and Engineering, The Nelson Mandela African Institution of Science and Technology (NM-AIST), P.O. Box 447, Nelson Mandela Rd, Tengeru, Arusha, Tanzania.

Citation information

Cite this article as: Molecular clusters Cs3X3 and Cs4X4 (X = Br, I): Quantum chemical study of structure and thermodynamic properties, Stanley F. Mwanga, Tatiana P. Pogrebnaya & Alexander M. Pogrebnoi, *Cogent Chemistry* (2016), 2: 1186582.

References

Badawi, M., Xerri, B., Canneaux, S., Cantrel, L., & Louis, F. (2012). Molecular structures and thermodynamic properties of 12 gaseous cesium-containing species of nuclear safety interest: Cs2, CsH, CsO, Cs2O, CsX, and Cs2X2 (X=OH, Cl, Br, and I). *Journal of Nuclear Materials, 420*, 452–462. http://dx.doi.org/10.1016/j.jnucmat.2011.10.034

Becke, A. D. (1993). Density-functional thermochemistry. III. The role of exact exchange. *The Journal of Chemical Physics, 98*, 5648–5652. http://dx.doi.org/10.1063/1.464913

Bencze, L., Lesar, A., & Popovic, A. (1998). The evaporation thermodynamics of lithium iodide. Mass spectrometric and *ab initio* studies. *Rapid Communications in Mass Spectrometry, 12*, 917–930. http://dx.doi.org/10.1002/(ISSN)1097-0231

Benson, S. W., & Patterson, M. J., (2009). *NASA's evolutionary xenon thruster (NEXT) ion propulsion technology development status in, (2009)*. Paper presented at the 31st International Electric Propulsion Conference, IEPC Paper, Ann Arbor, MI.

Bode, B. M., & Gordon, M. S. (1998). Macmolplt: A graphical user interface for GAMESS. *Journal of Molecular Graphics and Modelling, 16*, 133–138. http://dx.doi.org/10.1016/S1093-3263(99)00002-9

Boys, S. F., & Bernardi, F. (1970). The calculation of small molecular interactions by the differences of separate total energies. Some procedures with reduced errors. *Molecular. Physics, 19*, 553–566. http://dx.doi.org/10.1080/00268977000101561

Butman, M., Kudin, L., Smirnov, A., & Munir, Z. (2000). Mass spectrometric study of the molecular and ionic sublimation of cesium iodide single crystals. *International*

Journal of Mass Spectrometry, 202, 121–137. http://dx.doi.org/10.1016/S1387-3806(00)00232-3

Chupka, W. A. (1959). Dissociation energies of some gaseous alkali halide complex ions and the hydrated ion $K(H_2O)^+$. *The Journal of Chemical Physics, 30*, 458–465. http://dx.doi.org/10.1063/1.1729974

Cohen, A. J., & Gordon, R. G. (1975). Theory of the lattice energy, equilibrium structure, elastic constants, and pressure-induced phase transitions in alkali-halide crystals. *Physical Review B, 12*, 3228–3241. http://dx.doi.org/10.1103/PhysRevB.12.3228

Curtiss, L. A., Redfern, P. C., & Frurip, D. J. (2000). Theoretical methods for computing enthalpies of formation of gaseous compounds. *Reviews in Computational Chemistry, 15*, 147–211. http://dx.doi.org/10.1002/SERIES6143

Dunaev, A. M., Kudin, L. S., Butman, M. F., & Motalov, V. B. (2013). Alkali halide work function determination by Knudsen effusion mass spectrometry. *The Electrochemical Society Transactions, 46*, 251–258. doi:10.1149/04601.0251ecst

Fedorov, D. G., Koseki, S., Schmidt, M. W., & Gordon, M. S. (2003). Spin-orbit coupling in molecules: Chemistry beyond the adiabatic approximation. *International Reviews in Physical Chemistry, 22*, 551–592. http://dx.doi.org/10.1080/0144235032000101743

Granovsky, A. (2012). *Firefly version 8.1.0*. Retrieved from http://classic.chem.msu.su/gran/firefly/index.html

Groen, C. P., & Kovács, A. (2010). Matrix-isolation FT-IR study of $(CsBr)_n$ and $(CsI)_n$ (n=1–3). *Vibrational Spectroscopy, 54*, 30–34. http://dx.doi.org/10.1016/j.vibspec.2010.06.001

Gurvich, L. V., Yungman, V. S., Bergman, G. A., Veitz, I. V., Gusarov, A. V., Iorish, V. S., … Shenyavskaya, E. A. (2000). *Thermodynamic properties of individual substancvtanthes. Iermo for windows database on thermodynamic properties of individual substances and thermodynamic modeling software (1992–2000)* (Version 3.0). Moscow: Glushko Thermocenter of RAS.

Gusarov, A. V. (1986). *Equilibrium ionization in vapors of inorganic compounds and the thermodynamic properties of ions* (chemical sciences doctoral dissertation). All-Union Research Center of Surfaces and Vacuum (VNITsPV), Moscow.

Hishamunda, J., Girabawe, C., Pogrebnaya, T., & Pogrebnoi, A. (2012). Theoretical study of properties of Cs_2Cl^+, $CsCl_2^-$, $Cs_3Cl_2^+$, and $Cs_2Cl_3^-$ ions: Effect of basis set and computation method. *Rwanda Journal, 25*, 66–85.

Kay, T. P. (2011). *Magnetohydrodynamic energy conversion device using solar radiation as an energy source*. US Patent No. US 7982343 B2.

Lee, C., Yang, W., & Parr, R. G. (1988). Development of the Colle-Salvetti correlation-energy formula into a functional of the electron density. *Physical Review B, 37* 785–789. http://dx.doi.org/10.1103/PhysRevB.37.785

Lee, C.-J., Han, J.-I., Choi, D.-K., & Moon, D.-G. (2010). Transparent organic light-emitting devices with CsCl capping layers on semitransparent Ca/Ag cathodes. *Materials Science and Engineering: B, 172*, 76–79. http://dx.doi.org/10.1016/j.mseb.2010.04.020

Leininger, T., Nicklass, A., Küchle, W., Stoll, H., Dolg, M., & Bergner, A. (1996). The accuracy of the pseudopotential approximation: Non-frozen-core effects for spectroscopic constants of alkali fluorides XF (X = K, Rb, Cs). *Chemical Physics Letters, 255* , 274–280. http://dx.doi.org/10.1016/0009-2614(96)00382-X

Lennart, D., & Kjell, J. (1994). *Specific features of cesium chemistry and physics affecting reactor accident source term predictions*. Issy-les-Moulineaux: Organisation for Economic Co-Operation and Development-Nuclear Energy Agency, Committee on the Safety of Nuclear

Installations-OECD/NEA/CSNI.

Liao, Y.-X., Liu, J., Wang, B., & Yi, F.-T. (2011). Multiform structures with silicon nanopillars by cesium chloride self-assembly and dry etching. *Applied Surface Science, 257*, 10489–10493. http://dx.doi.org/10.1016/j.apsusc.2011.07.014

Liu, J., Ashmkhan, M., Dong, G., Wang, B., & Yi, F. (2013). Fabrication of micro-nano surface texture by CsCl lithography with antireflection and photoelectronic properties for solar cells. *Solar Energy Materials and Solar Cells, 108*, 93–97. http://dx.doi.org/10.1016/j.solmat.2012.09.016

Liu, W., Ferguson, M., Yavuz, M., & Cui, B. (2012). Porous TEM windows fabrication using CsCl self-assembly. *Journal of Vacuum Science & Technology B, 30*, 06F201.

Liu, Y., Zhao, J., Li, F., & Chen, Z. (2013). Appropriate description of intermolecular interactions in the methane hydrates: An assessment of DFT methods. *Journal of Computational Chemistry, 34*, 121–131. http://dx.doi.org/10.1002/jcc.23112

Martin, J. M., & Sundermann, A. (2001). Correlation consistent valence basis sets for use with the Stuttgart–Dresden–Bonn relativistic effective core potentials: The atoms Ga–Kr and In–Xe. *The Journal of Chemical Physics, 114*, 3408–3420. http://dx.doi.org/10.1063/1.1337864

Mwanga, S. F., Pogrebnaya, T. P., & Pogrebnoi, A. M. (2015a). Structure and properties of molecular and ionic clusters in vapour over caesium fluoride. *Molecular Physics, 113*, 1485–1500. doi:10.1080/00268976.2015.1007104

Mwanga, S. F., Pogrebnaya, T. P., & Pogrebnoi, A. M. (2015b). Theoretical study of cluster ions existing in vapours over cesium bromide and iodide. *British Journal of Applied Science & Technology, 9*, 108–130. doi:10.9734/BJAST/2015/17612

Mwanga, S. F., Pogrebnaya, T. P., & Pogrebnoi, A. M. (2016). Molecular and ionic clusters existing in vapor over cesium chloride: Structure and thermodynamic properties. *Computational and Theoretical Chemistry, 1078*, 47–54. doi:10.1016/j.Comptc.2015.12.013

Pogrebnaya, T. P., Hishamunda, J. B., Girabawe, C., & Pogrebnoi, A. M. (2012). Theoretical study of structure, vibration spectra and thermodynamic properties of cluster ions in vapors over potassium, rubidium and cesium chlorides. In *Chemistry for sustainable development* (Chap. 21, pp. 353–366). Dordrecht: Springer.

Pogrebnaya, T., Pogrebnoi, A., & Kudin, L. (2008). Calculation of the thermodynamic characteristics of ions in vapor over sodium fluoride. *Russian Journal of Physical Chemistry A, 82*, 75–82. http://dx.doi.org/10.1134/S0036024408010111

Pogrebnoi, A. M., Kudin, L. S., & Kuznetsov, A. Y. (2000). Enthalpies of formation of the ions present in the saturated vapor over cesium chloride. *Russian Journal of Physical Chemistry, 74*, 1728–1730.

Povinec, P. P., Aoyama, M., Biddulph, D., Breier, R., Buesseler, K., Chang, C., … Jull, A. (2013). Cesium, iodine and tritium in NW Pacific waters - A comparison of the Fukushima impact with global fallout. *Biogeosciences, 10*, 5481–5496. http://dx.doi.org/10.5194/bg-10-5481-2013

Roki, F., Ohnet, M., Fillet, S., Chatillon, C., & Nuta, I. (2013). Knudsen cell mass spectrometric study of the Cs2IOH(g) molecule thermodynamics. *The Journal of Chemical Thermodynamics, 65*, 247–264. http://dx.doi.org/10.1016/j.jct.2013.05.032

Roki, F.-Z., Ohnet, M.-N., Fillet, S., Chatillon, C., & Nuta, I. (2014). Critical assessment of thermodynamic properties of CsI solid, liquid and gas phases. *The Journal of Chemical Thermodynamics, 70*, 46–72. http://dx.doi.org/10.1016/j.jct.2013.09.038

Rupp, M., & Ahlrichs, R. (1977). Theoretical investigation of structure and stability of oligomers of LiH, NaH, LiF, and NaF. *Theoretica Chimica Acta, 46*, 117–127. http://dx.doi.org/10.1007/BF00548087

Schmidt, M. W., Baldridge, K. K., Boatz, J. A., Elbert, S. T., Gordon, M. S., Jensen, J. H., ... Montgomery, J. A. (1993). General atomic and molecular electronic structure system. *Journal of Computational Chemistry, 14*, 1347–1363. doi:10.1002/jcc.540141112

Schuchardt, K. L., Didier, B. T., Elsethagen, T., Sun, L., Gurumoorthi, V., Chase, J., ... Windus, T. L. (2007). Basis set exchange: A community database for computational sciences. *Journal of Chemical Information and Modeling, 47*, 1045–1052. doi:10.1021/ci600510j

Sidorova, I., Gusarov, A., & Gorokhov, L. (1979). Ion-molecule equilibria in the vapors over cesium iodide and sodium fluoride. *International Journal of Mass Spectrometry and Ion Physics, 31*, 367–372. doi:10.1016/0020-7381(79)80073-X

Snelson, A. (1967). Infrared spectrum of LiF, Li2F2, and Li3F3 by matrix isolation. *The Journal of Chemical Physics, 46*, 3652–3656. http://dx.doi.org/10.1063/1.1841269

Solomonik, V. G., Smirnov, A. N., & Mileev, M. A. (2005). Structure, vibrational spectra, and energetic stability of

LnX_4^- (Ln = La, Lu; X = F, Cl, Br, I) ions. *Koordinatsionnaya Khimiya, 31*, 218–228.

Tokarev, K. L. (2007–2009). *OpenThermo* (v.1.0 Beta 1 (C) ed.).

Weis, P., Ochsenfeld, C., Ahlrichs, R., & Kappes, M. M. (1992). Ab initio studies of small sodium–sodium halide clusters, Na_nCl_n and Na_nCl_{n-1} (n≤4). *The Journal of Chemical Physics, 97*, 2553–2560. http://dx.doi.org/10.1063/1.463094

Welch, D., Lazareth, O., Dienes, G., & Hatcher, R. (1976). Alkali halide molecules: Configurations and molecular characteristics of dimers and trimers. *The Journal of Chemical Physics, 64*, 835–839. http://dx.doi.org/10.1063/1.432231

Zhang, X., Liu, J., Wang, B., Zhang, T., & Yi, F. (2014). Fabrication of silicon nanotip arrays with high aspect ratio by cesium chloride self-assembly and dry etching. *AIP Advances, 4*, 031335. http://dx.doi.org/10.1063/1.4869238

Zhang, Y., Li, J., Wei, T., Liu, J., Yi, X., Wang, G., & Yi, F. (2012). Enhancement in the light output power of GaN-based light-emitting diodes with nanotextured indium tin oxide layer using self-assembled cesium chloride nanospheres. *Japanese Journal of Applied Physics, 51*, 020204. http://dx.doi.org/10.7567/JJAP.51.020204

Zhurko, G., & Zhurko, D. (2014). *Chemcraft* (version 1.7, build 382).